Journal of Statistical Physics, Vol. 54, Nos. 5/6, 1989

A Modified Pitchfork Bifurcation as a Model of the TI–TII Transition in Liquid Helium Counterflow with External Noise

Mark Schumaker[1] **and Werner Horsthemke**[2]

Received April 30, 1988; revision received August 6, 1988

An amended pitchfork bifurcation is introduced to model recent experiments by Griswold and Tough on superfluid turbulence in liquid helium counterflow subject to strong external noise. We adopt the generalized white noise limit of Blankenship and Papanicolaou to take a short-correlation-time limit of the nonlinear noise which enters into the model, and we implement this limit by means of the wideband perturbation expansion. Novel boundary conditions are applied to the resultant diffusion process in order to obtain behavior in qualitative agreement with the observations at low vortex line density. We are able to account for the sharp peak in probability observed experimentally at a small positive line density. The drift and diffusion of our diffusion process may be estimated experimentally; we describe how to do this.

KEY WORDS: Superfluid turbulence; pitchfork bifurcation; nonlinear noise.

1. INTRODUCTION

In this paper we discuss in some detail a phenomenological model developed to describe the TI–TII transition between superfluid turbulent states of liquid helium counterflow in the presence of deliberately applied external noise. For a broader description of this model as well as a description of an earlier model for intrinsic fluctuations in superfluid turbulence, see the companion paper.[1] Experiments on the liquid helium system were performed by Don Griswold and Jim Tough at Ohio State University.[2]

The experiments using external noise were a modification of earlier experiments performed by Griswold *et al.*[3] in which no external noise was

[1] Department of Chemistry, Brandeis University, Waltham, Massachusetts, 02254-9110.
[2] Ilya Prigogine Center for Studies in Statistical Mechanics, Department of Physics, University of Texas at Austin, Austin, Texas 78712-9990.

0022-4715/89/0300-1189$06.00/0

822/54/5-6-6

applied. In both sets of experiments the chemical potential $\Delta\mu$ across the counterflow tube was measured as a function of the rate of heat flow $\dot{Q}$ through the tube. $\Delta\mu$ is proportional to the vortex line density L in the counterflow tube. Even in the absence of deliberately applied noise, small fluctuations in the vortex line density were observed. Steady-state values of the vortex line density, the variance of fluctuations about these states, and the power of these fluctuations in a band of frequencies were all measured as a function of $\dot{Q}$.

We have developed a model for these measurements in the absence of deliberately applied external noise.[4] This model assumes that the TI–TII transition can be described as part of the unfolding of a pitchfork bifurcation. We were able to account qualitatively for the measured steady states, the variance about those steady states, and the power in the fluctuations.

Below we describe a more recently developed model for the experiments performed in the presence of deliberately applied external noise. The unfolding of the pitchfork bifurcation is still used, but we have to modify it in order to take into account the fact that the external noise brings global features of the state and parameter spaces into play. We first describe the model, which initially has two state variables. In order to proceed with the analysis, we take a short-correlation-time limit and reduce the model to only a single state variable. This reduction faces a technical difficulty because the applied noise enters into the model in a nonlinear way. However, we are able to take the generalized white noise limit of Blankenship and Papanicolaou.[5] This limit is implemented by means of the wideband perturbation expansion.[6] In this way we obtain a reduced Fokker–Planck equation in a single state variable. We describe the "reinjection" boundary condition that has been assumed, and show how our model accounts for a somewhat mysterious feature of the experimental data: namely, that the external noise actually enhances the probability at low vortex line density. We finally show how the key quantities in this model may be measured experimentally.

2. THE MODIFIED PITCHFORK MODEL

Figure 1 sketches the steady states of the imperfect pitchfork model in the neighborhood of the TI–TII transition. The experimental coordinates $(\dot{Q}, L^{1/2})$ are shown in relation to the model control parameter λ and state variable x. The two coordinate systems are related obliquely, with coordinate transformations given by

$$x = L^{1/2} - s\dot{Q} + b \tag{2.1a}$$

$$\lambda = \dot{Q} - \dot{Q}_0 \tag{2.1b}$$

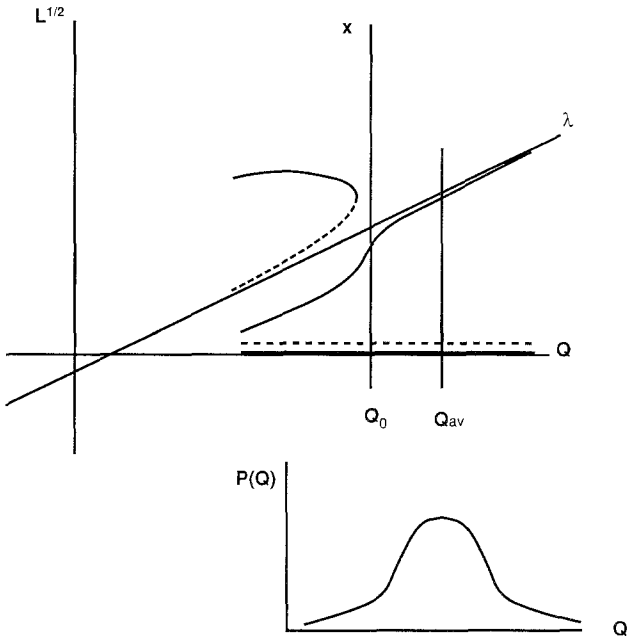

Fig. 1. The qualitative nature of oblique noise in relation to the experimental and normal form coordinate systems. Oblique noise is due to fluctuations of the heat current $\dot{Q}$, which has an average value $\dot{Q}_{av}$. In the model the fluctuations are assumed to follow an Ornstein–Uhlenbeck process z, which has a Gaussian stationary probability density sketched in the bottom diagram.

Here s is the slope of the λ axis relative to the experimental coordinate system, $-b$ is the $L^{1/2}$ intercept of the λ axis, and $\dot{Q}_0$ is the value of the heat current at the origin of the normal form coordinate system.

Also indicated in Fig. 1 is the average value of the heat current $\dot{Q}_{av}$ when fluctuations on the heat current are deliberately imposed. The extent of these fluctuations is suggested by the probability distribution sketched below. Geometrically, the fluctuating heat current can be thought of as carrying the system back and forth along the $\dot{Q}$ axis in the figure. While this effect is quite simple from the point of view of the experimental coordinates, we see that it is somewhat less trivial in the frame of reference of the model coordinates. The noise acts obliquely relative to the latter coordinate system, mixing values of x and λ. We shall therefore refer to it as "oblique noise." When this noise is transformed by Eq. (2.1), it will have a highly nonlinear character in the (λ, x) coordinate system. This nonlinearity makes the analysis of this problem very interesting from the point of view of stochastic methods.

Formally, it will be very easy to introduce noise into the dynamical

equation for the state variable x. Let the random fluctuations in the heat current $\dot{Q}$ be modeled by the Ornstein–Uhlenbeck process z. Then if the dynamical equations are expressed in terms of the experimental variables, the introduction of oblique noise corresponds to substituting for the variable $\dot{Q}$ the expression $\dot{Q}_{\text{av}} + z$. The state variable $L^{1/2}$ is not changed directly by the heat current fluctuations, and therefore the dependence of the dynamical equations on $L^{1/2}$ remains unchanged. Transforming according to Eq. (2.1), we find that for equations written in terms of x and λ we must make the substitutions

$$\lambda \to \bar{\lambda} + z, \qquad x \to x - sz \tag{2.2}$$

The dynamical equation for the strong-noise case is based on the imperfect pitchfork bifurcation which we introduced previously.[4] However, we are now concerned with external noise which involves a large range of heat currents $\dot{Q}$ and spreads the probability distribution for the system over a wide interval in the domain of the state variable. The dynamics is no longer dependent on only the local character of the TI–TII transition; global aspects of the system now come into play. While our dynamical equation is still based on the pitchfork bifurcation, it is amended in several ways. This modified dynamical equation has the form

$$\dot{x} = k(L^{1/2})\, m(\lambda)\, p(x, \lambda) \tag{2.3}$$

Consider the term $p(x, \lambda)$, the universal unfolding of the pitchfork bifurcation. We now write this as

$$p(x, \lambda) = \beta_0 + \beta_1 \lambda x + \beta_2 x^2 + \beta_3 x^3 \tag{2.4}$$

As compared with the unfolding given previously,[4] we have introduced two additional coefficients: β_0 and β_3. One degree of freedom is introduced to allow the relative scaling of the λ and x axis to be arbitrary; this will permit us to scale these axis with the same units as are used to scale $\dot{Q}$ and $L^{1/2}$. The second degree of freedom allows us to scale the relaxation time $[\partial_x p(x_{\text{ss}}, \lambda)]^{-1}$ without changing the steady states. Here x_{ss} is a solution of $p(x_{\text{ss}}, \lambda) = 0$, and is therefore a steady state of (2.3).

The factor $k(L^{1/2})$ is the mechanism by which we introduce the laminar steady state and the unstable steady state that must exist between the turbulent and laminar steady states. It is known from experiment that the counterflow system can be maintained in a metastable laminar state (corresponding to zero vortex line density) well past the critical heat current of the TI–TII transition. The corresponding steady state in our

model must come from a zero of $k(L^{1/2})\, m(\lambda)\, p(x, \lambda)$ when $L^{1/2} = 0$; this zero is supplied by $k(L^{1/2})$, which has the form

$$k(L^{1/2}) = 1 - \mathrm{Lor}(L^{1/2}) \tag{2.5}$$

with the Lorentzian

$$\mathrm{Lor}(L^{1/2}) = \frac{a}{1 + (L^{1/2} - L_0^{1/2})^2 / w^2}$$

The constants a, w, and $L_0^{1/2}$ are chosen so that $\mathrm{Lor}(L^{1/2}) = 1$ has two roots, one at $L_{1/2} = 0$ and the other at $L^{1/2} = 2L_0^{1/2}$. For $L^{1/2}$ sufficiently large, $k(L^{1/2})$ approaches 1 asymptotically, leaving the dynamics in (2.3) dependent on $m(\lambda)\, p(x, \lambda)$. This latter expression is positive for values of x less than that of the turbulent steady states, reflecting the fact that the steady states pull trajectories up toward them. The zero at $L^{1/2} = 2L_0^{1/2} = L_u^{1/2}$ corresponds to an unstable steady state. For $L^{1/2} > L_u^{1/2}$ we have $k(L^{1/2}) > 0$, giving a drift that is positive and directed away from the unstable steady state. For $L^{1/2} < L_u^{1/2}$ we have $k(L^{1/2}) < 0$, and the drift pulls trajectories toward the laminar state at $L^{1/2} = 0$. Since $k(L^{1/2})$ is not a function of λ, its zeros at $L^{1/2} = 0$ and $L^{1/2} = L_u^{1/2}$ are not dependent on λ either. This lack of dependence on λ is obviously appropriate for the laminar state, which corresponds to a state of zero vortex line density regardless of $\dot{Q}$, so long as it exists. It should also be a fair approximation for the unstable steady state for the following reason. As $\dot{Q}$ increases from the critical heat current $\dot{Q}_1$ at the initial bifurcation to turbulence, the branch of unstable steady states emanating from the saddle-node bifurcation initially curves down toward lower values of $L^{1/2}$. For increasing $\dot{Q}$ the turbulent steady state becomes more stable, and it seems natural to assume that the curve of unstable steady states approaches lower values of $L^{1/2}$. However, the metastable laminar state continues to exist, so the curve of unstable states must approach the axis $L^{1/2} = 0$ with decreasing slope, and eventually run almost parallel to it. The additional roots corresponding to the metastable laminar state and the associated unstable steady state are also shown in Fig. 1.

Our introduction of a factor $m(\lambda)$ is motivated by the measured relaxation times to the turbulent steady states of the counterflow system in the neighborhood of the TI–TII transition (ref. 7, Fig. 64). These measurements were taken in the absence of external noise, yet we will see that they are important in our understanding of the system in the presence of external noise. In order to introduce the qualitative character of these relaxation times into our model, the factor $m(\lambda)$ must bias the system toward greater relaxation times as λ increases. $m(\lambda)$ has the general form

$$m(\lambda) = 1 + \alpha_0 \lambda + \alpha_2 \lambda^2 \tag{2.6}$$

Below, we show a calculation for a general quadratic $m(\lambda)$ and choose for the model a parabola that has value 1 at $\lambda = 0$ ($\dot{Q} = 118.78$) and reaches a minimum of 0 at $\lambda = 161.22$ ($\dot{Q} = 280$). The model relaxation times are proportional to $m(\lambda)^{-1}$, and will ultimately increases as $m(\lambda) \downarrow 0$. Unfortunately, with a simple quadratic $m(\lambda)$, we cannot obtain good quantitative agreement between the model relaxation times and the measured ones. Nevertheless, the positive bias in the relaxation time enables us to find in the model the noisy hysteresis curve which is an important result of Griswold and Tough's experiments. Without the factor $m(\lambda)$ the system $\dot{x} = k(L^{1/2})\, p(x, \lambda)$ does not display this feature.

3. WIDE BAND PERTURBATION EXPANSION

After introducing oblique noise into our dynamical equation by substituting the expressions given in (2.2) for x and λ in (2.3), we obtain a new set of dynamical equations in the two state variables x and z. These equations have the form

$$dx = H(x, z)\, dt \tag{3.1a}$$

$$dz = -\gamma z\, dt + \sigma\, dW(t) \tag{3.1b}$$

where

$$H(x,z) = b_0 + b_1 z + b_2 z^2 + b_3 z^3 + b_4 z^4 + b_5 z^5 \tag{3.1c}$$

and the b_i are functions of x: $b_i = b_i(x)$, $1 \leqslant i \leqslant 5$. In general it is difficult to make progress in the analysis of a stochastic differential equation, such as (3.1), in two state variables. For example, we would like to solve for the stationary probability distribution, but this is in general not possible for a two-variable system. However, the stationary probability distribution can always be found, when it exists, for a stochastic differential equation in a single state variable.

Fortunately, the system (3.1) can be reduced to a single state variable by the application of a short-correlation-time limit. We use the generalized white noise limit of Blankenship and Papanicolaou.[5] It is closely related to the ordinary white noise limit; however, it is more general and can be applied to the analysis of nonlinear noise. The procedure by which we take this limit is called the "wide band perturbation expansion" and was developed by Horsthemke and Lefever.[6]

The qualitative ideas behind the generalized limit are the following. A short-correlation-time limit is taken which, if the amplitude were held constant, would lead to no noise at all. To keep the variance in response to the

noise nonzero, the amplitude of the noise must be scaled up appropriately as the short-correlation-time limit is taken. Finally, we have the step that generalizes the usual white noise limit: the mean value of the noise must be subtracted out before the amplitude is scaled up, keeping the variance of the system in response to the noise finite. In the case of a linear dependence on the Ornstein–Uhlenbeck noise z, the mean value is zero and the last step would be unnecessary. Applying all of these considerations, we obtain the following pair process, depending on the small parameter ε:

$$dx = E_z[H(x, z)]\, dt + \frac{1}{\varepsilon}\{H(x, z) - E_z[H(x, z)]\}\, dt \tag{3.2a}$$

$$dz = -\frac{1}{\varepsilon^2}\gamma z\, dt + \frac{1}{\varepsilon}\sigma\, dW \tag{3.2b}$$

It is convenient to define the renormalized functions $F(x)$ and $G(x, z)$ in such a way that $E_z[G(x,z)] = 0$:

$$F(x) = E_z[H(x, z)] \tag{3.3a}$$

$$G(x, z) = H(x, z) - E_z[H(x, z)] \tag{3.3b}$$

The Fokker–Planck equation associated with the process (3.2) has the form

$$\partial_t P(x, z) = \left(\frac{1}{\varepsilon^2}F_1 + \frac{1}{\varepsilon}F_2 + F_3\right) P(x, z) \tag{3.4}$$

where

$$F_1 = -\gamma\, \partial_z z + \frac{1}{2}\sigma^2\, \partial_{zz} \tag{3.5}$$

$$F_2 = -\partial_x G(x, z) \tag{3.6}$$

$$F_3 = -\partial_x F(x) \tag{3.7}$$

Note that F_1 is the Fokker–Planck operator for the Ornstein–Uhlenbeck process and involves the variable z alone. F_3 involves x alone and F_2 contains the cross terms. Now we expand the probability density as a series of terms in the smallness parameter ε:

$$P(x, z, t) = P_0(x, z, t) + \varepsilon P_1(x, z, t) + \varepsilon^2 P_2(x, z, t) + \cdots \tag{3.8}$$

Introducing the expansion (3.8) into the Fokker–Planck equation (3.4) and

equating terms of the same order in ε, we get an infinite hierarchy of equations:

$$\varepsilon^{-2}: \quad 0 = F_1 P_0 \tag{3.9}$$

$$\varepsilon^{-1}: \quad 0 = F_1 P_1 + F_2 P_0 \tag{3.10}$$

$$\varepsilon^{0}: \quad \partial_t P_0 = F_1 P_2 + F_2 P_1 + F_3 P_0 \tag{3.11}$$

$$\varepsilon^{k}: \quad \partial_t P_k = F_1 P_{k+2} + F_2 P_{k+1} + F_3 P_k, \qquad k \geqslant 1 \tag{3.12}$$

Equation (3.9) implies that P_0 solves the time-independent Fokker–Planck equation for the Ornstein–Uhlenbeck process, and therefore the z dependence of P_0 is just a Gaussian stationary probability density. We can write P_0 in the separated form

$$P_0(x, z, t) = r_0(x, t)\, p_s(z) \tag{3.13}$$

Physically this means that in the limit of zero correlation time the state of the noise process and the state of the system become independent. Notice that we do not know the form for $r_0(x, t)$; this will be obtained later in the analysis of order ε^0.

For the higher order terms we shall define

$$P_k(x, z, t) = r_k(x, z, t)\, p_s(z), \qquad k \geqslant 1 \tag{3.14}$$

This definition can always be made, since $p_s(z)$ is an everywhere positive function. Note that for $k \geqslant 0$, $r_k(x, z, t)$ depends in general on z.

Now we go on to order ε^{-1}, where we must solve (3.10). A simple calculation shows that the solvability condition is automatically satisfied. We can therefore solve the order ε^{-1} equation, which may be rewritten as

$$F_1^+ r_1 = \partial_x G(x, z)\, r_0(x, t) \tag{3.15}$$

where F_1^+ is the adjoint of F_1:

$$F_1^+ = \gamma z\, \partial_z + \frac{1}{2}\sigma^2\, \partial_{zz} \tag{3.16}$$

Equation (3.15) is one of the two important results we need. It will be used to solve for r_1 in terms of r_0, and close the reduced Fokker–Planck equation for r_0. To obtain this latter equation, we must go on to order ε^0.

The solvability condition for order ε^0 turns out to be

$$0 = \int_{-\infty}^{+\infty} p_s(z)(\partial_t r_0 - F_2 r_1 - F_3 r_0)\, dz \tag{3.17}$$

This is the second important result we need. We use (3.15) to solve for r_1 in terms of r_0 and then insert the result in (3.17). After carrying out the integration, we then cast (3.17) in the form of a Fokker–Planck equation for r_0.

After a substantial calculation, we finally have for the reduced Fokker–Planck equation:

$$\partial_t r_0 = -\partial_x [f_d(x) + f_n(x) + f_I(x)]\, r_0 + \frac{1}{2}\partial_{xx} g_I^2 r_0 \tag{3.18}$$

where

$$f_d(x) = k(L^{1/2})\, m(\bar{\lambda})\, p(x, \bar{\lambda}) \tag{3.19}$$

$$f_n(x) = b_2(x)\, v + 3b_4(x)\, v^2 \tag{3.20}$$

$$f_I(x) = \frac{1}{2}\, g_I \partial_x\, g_I \tag{3.21}$$

and

$$\begin{aligned} g_I^2 = \frac{1}{\gamma} (&2v^2 b_1^2 + 12v^2 b_1 b_3 + 2v^2 b_2^2 + 60v^3 b_1 b_5 \\ &+ 22v^3 b_3^2 + 24v^3 b_2 b_4 + 260v^4 b_3 b_5 \\ &+ 84v^4 b_4^2 + 898v^5 b_5^2) \end{aligned} \tag{3.22}$$

The term f_d is simply the deterministic dynamics at heat current $\bar{\lambda}$, the average value of λ. The second term f_n is a systematic effect due to the noise which we separated from the diffusion term before we took the short-correlation-time limit (3.2). It is an effect due to the nonlinear nature of the noise; no similar term appears on taking the white noise limit of a linear noise process. The third component of the drift is f_I, which has the form of a noise-induced drift due to the diffusion g_I^2. This is the same noise-induced drift that appears in the Fokker–Planck equation written down for a Stratonovich stochastic differential equation. It represents the first correction taking into account the finite correlation time of the noise. However, unlike the result for linear noise, we see that f_I and g_I^2 are both proportional to γ^{-1}. The finite correlation time of the original noise process appears explicitly in the reduced Fokker–Planck equation.

The reduced Fokker–Planck equation (3.18) is not yet a satisfactory model for the oblique noise process because the unstable steady state $L_u^{1/2}$ is a natural boundary. $L_u^{1/2}$ is a natural boundary because it is a root of $k(L^{1/2})$, which is itself a factor of both the drift and diffusion in Eq. (3.18).

Therefore both the drift and diffusion go to zero at $L_u^{1/2}$; realizations will not be able to pass from one side of $L_u^{1/2}$ to the other, and the state space is partitioned into two pieces. However, in the physical system the unstable steady state does not represent an absolute barrier. Certainly it will not lie precisely parallel to the $\dot{Q}$ axis, so that it would be possible for the oblique noise to take the system from one side of $L_u^{1/2}$ to the other. In addition, we know that internal fluctuations are present: this would also allow realizations to cross the unstable state.

A way to prevent $L_u^{1/2}$ from becoming an absolute barrier in the model is to add a term into the diffusion which does not go to zero with $k(L^{1/2})$. It suffices to introduce an independent additive noise σ_i^2. The reduced Fokker–Planck equation for the stationary probability density then becomes

$$0 = -\partial_x[f_d(x) + f_n(x) + f_I(x)]\, r_0 + \frac{1}{2}\partial_{xx}[g_I^2(x) + \sigma_i^2]\, r_0 \qquad (3.23)$$

4. THE REINJECTION PROBABILITY DENSITY

Griswold and Tough made careful measurements of the probability density close to the regime of zero line density in the presence of oblique noise. They found that the probability always decreases to zero at the laminar state, even though in many cases it reaches a very sharp maximum at a low vortex line density very close to the laminar state. We are faced with some difficulty in reconciling this result with the knowledge that the laminar state is metastable and the nature of the external noise. This difficulty is due to the fact that random variations of $\dot{Q}$ in the laminar state just take the system from one (meta) stable state to another. Without some additional feature in the dynamics, it is hard to see how the laminar state is destabilized. The physical basis for the instability of the laminar state in the presence of moderate fluctuations in the heat current is unknown.

From the point of view of our phenomenological model, however, there is only one way to accomplish the instability and retain our interpretation of the laminar state as corresponding to zero integrated vortex line density between the two ends of the flow tube. Once a realization reaches the laminar state $L^{1/2} = 0$, which is a boundary of the state space, it must be reinjected elsewhere in the state space. The simplest possibility for the purpose of our model is that the probability is sent to the other boundary of the state space, at some positive vortex line density. A possible physical interpretation is that a new dynamical mechanism comes into play when the counterflow system approaches the laminar state too closely. This new mechanism generates vortex line density on a short time scale com-

pared to the evolution of the probability density in the interior of the state space.

We therefore seek to construct a diffusion process with the following boundary conditions. When the sample paths reach the boundary at $L^{1/2}=0$, corresponding to the stable laminar steady state, they are immediately reinjected into the state space at the boundary $L^{1/2}=c$, corresponding to the arbitrary upper limit of vortex line density. When trajectories reach the boundary at $L^{1/2}=c$, they merely reflect off the boundary. These boundary conditions are depicted in Fig. 2, and we shall now find the formula for the corresponding stationary probability density. This problem is a limiting case of a random process discussed by Karlin and Taylor.[8] We begin by describing the situation that they consider.

Karlin and Taylor analyze the "instantaneous return process," a diffusion process whose state space is the interval $a \leqslant \xi \leqslant b$ with state variable ξ. Whenever a sample path reaches either boundary it instantaneously returns to its starting point $x_0 \in (a, b)$. The stationary probability density for this process is shown to be given by

$$\alpha(\xi)=\frac{\mathcal{G}(x_0, \xi)}{\int_a^b \mathcal{G}(x_0, \eta)\, d\eta} \tag{4.1}$$

where the Green function $\mathcal{G}(x, \xi)$ is given by

$$\mathcal{G}(x, \xi)=\begin{cases}\mathcal{G}_>(x, \xi) & \text{when } \xi \geqslant x \\ \mathcal{G}_<(x, \xi) & \text{when } \xi \leqslant x\end{cases} \tag{4.2}$$

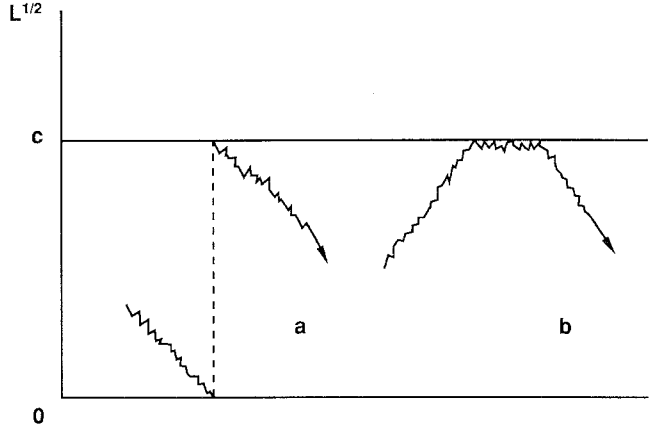

Fig. 2. Sample paths of the model diffusion process for reinjection boundary conditions. The abscissa is time and the ordinate shows the state space $[0, c]$ of the diffusion process. (i) The boundary $L^{1/2}=0$ is the reinjection boundary. Once a realization attains $L^{1/2}=0$ it is immediately reintroduced at $L^{1/2}=c$. (ii) The boundary $L^{1/2}$ is a reflection boundary. Sample paths that would otherwise cross the boundary are reflected as if by a mirror.

with

$$\mathcal{G}_>(x,\xi) = 2\frac{[S(x)-S(a)][S(b)-S(\xi)]}{S(b)-S(a)}\frac{1}{\sigma^2(\xi)\,s(\xi)} \tag{4.3}$$

$$\mathcal{G}_<(x,\xi) = 2\frac{[S(b)-S(x)][S(\xi)-S(a)]}{S(b)-S(a)}\frac{1}{\sigma^2(\xi)\,s(\xi)} \tag{4.4}$$

and

$$S(x) = \int^x s(\xi)\,d\xi \tag{4.5}$$

$$s(\xi) = \exp\left\{-\int^\xi \frac{2f(\eta)}{g^2(\eta)}\,d\eta\right\} \tag{4.6}$$

Here $f(x)$ denotes the drift and $g^2(x)$ denotes the diffusion of this random process. $S(x)$ and $s(\xi)$ are deliberately defined as indefinite integrals.

We focus on the probability density for $\xi < x_0$. This is given by

$$\alpha_<(\xi) = \frac{\mathcal{G}_<(x_0,\xi)}{\int_a^{x_0}\mathcal{G}_<(x_0,\eta)\,d\eta + \int_{x_0}^b \mathcal{G}_>(x_0,\eta)\,d\eta} \tag{4.7}$$

In the limit as $x_0 \uparrow b$ this density converges to the one desired for reinjection boundary conditions. When realizations reach the left-hand endpoint a $(=0)$ they are instantaneously returned to the right-hand endpoint b $(=c)$. Suppose now that $x_0 = b-\varepsilon$, where $\varepsilon \ll 1$, and examine the order in ε of the two integrals in the denominator of (4.7). For the integral over $\mathcal{G}_<$ we have

$$\int_a^{b-\varepsilon}\mathcal{G}_<(b-\varepsilon,\eta)\,d\eta = \int_a^{b-\varepsilon} d\eta\left[\varepsilon S'(b)\,2\frac{S(\eta)-S(a)}{S(b)-S(a)}\frac{1}{\sigma^2(\eta)\,s(\eta)} + O(\varepsilon^2)\right] \tag{4.8}$$

and we see that this is of order ε. Now consider the integral over $\mathcal{G}_>$:

$$\int_{b-\varepsilon}^b \mathcal{G}_>(b-\varepsilon,\eta)\,d\eta = \int_{b-\varepsilon}^b d\eta\,2\frac{[S(b-\varepsilon)-S(a)][S(b)-S(\eta)]}{S(b)-S(a)}\frac{1}{\sigma^2(\eta)\,s(\eta)} \tag{4.9}$$

But since $b-\varepsilon \leqslant \eta \leqslant b$ we have

$$S(b)-S(\eta) = (b-\eta)\,S'(b) + O((b-\eta)^2) = O(\varepsilon) \tag{4.10}$$

We see that in the expansion of (4.9) we will have one order of ε from the integrand and one order from the range of integration; therefore this

integral is of order ε^2. We also have that $\mathscr{G}_<$ is itself of order ε. Then the ratio (4.7) is finite in the limit as $\varepsilon \downarrow 0$, and in the denominator the integral over $\mathscr{G}_<$ dominates the integral over $\mathscr{G}_>$. We have for the stationary probability density P_s of our reinjection process

$$P_s(\xi) = \lim_{\varepsilon \downarrow 0} \frac{\mathscr{G}_<(c-\varepsilon, \xi)}{\int_0^{c-\varepsilon} \mathscr{G}_<(c-\varepsilon, \eta)\, d\eta} = \mathscr{N} \frac{S(\xi) - S(0)}{\sigma^2(\xi)\, s(\xi)} \tag{4.11}$$

where $\mathscr{N}$ is the normalization constant. Note that this result does have the general form for the stationary probability density of a diffusion process with nonzero probability current.[6] The result of (4.11) was integrated numerically to obtain the probability distributions and bifurcation diagrams for the model that will be compared in the next section with the experimental results.

5. MODEL RESULTS

Figure 3 shows a "bifurcation diagram" generated by the model. On the ordinate is the state variable for the noisy system: the extrema of the probability distributions $r_0(x)$ computed from the model Fokker–Planck equation (3.23). On the abscissa is the control parameter $\dot{Q}$. For a given value of the $\dot{Q}$, x can be regarded as a renormalized vortex line density $L^{1/2}$; recall (2.1a). The stationary probability distributions are given by formula (4.11), taking into account reinjection boundary conditions as discussed above. The functions f and g^2 introduced in (4.6) are $f(x) = f_d(x) + f_n(x) + f_I(x)$ and $g^2(x) = g_I^2(x) + \sigma_i^2$. The open circles in Fig. 3 correspond to maxima of the stationary probability distribution and the solid circles correspond to minima. The solid line drawn through the open circles and the dashed line drawn through the solid circles are meant to suggest the locus of extrema. Also shown as a solid line are the steady states of the model (2.3) in the absence of the noise term z. Values of model parameters used to construct this figure are given in the caption to Fig. 3.

Figure 3 may be compared in a preliminary way with the experimental results from Griswold and Tough[2] reproduced in Fig. 4. The square roots of the vortex line densities at which extrema appear in experimentally constructed probability distributions are plotted on the vertical axis. Here $L_m^{1/2}$ is the vortex line density associated with an extremum, and d ($=132\ \mu$m) is the diameter of the flow tube. On the abscissa is $\tilde{Q}$, the heat current normalized by its value at the *paracritical point*,[4] 121 μW. The comparison between Fig. 3 and 4 is not strict, however. The probability densities shown in Fig. 3 were constructed as a function of $L^{1/2}$, with the extrema measured from these. In contrast, the experimental probability densities associated

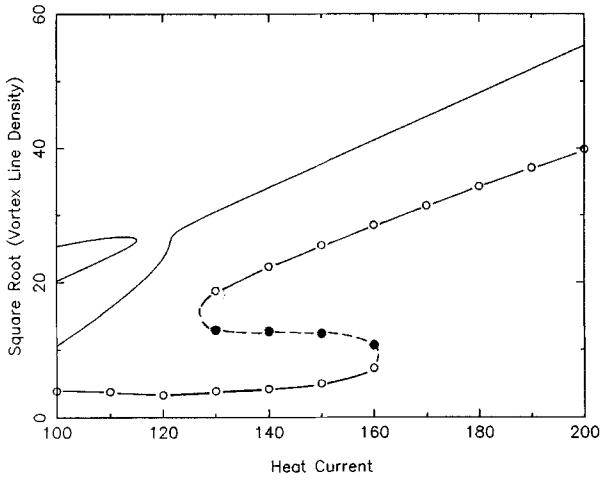

Fig. 3. Bifurcation diagrams constructed from the extrema of model probability densities. This figure was constructed with the following model parameter values. Oblique coordinate system parameters are $\dot{Q}_0 = 118.78$, $L_0^{1/2} = 26.717$, $s = 0.3529$. Pitchfork parameter values are $\beta_0 = 0.6687$, $\beta_1 = 0.375$, $\beta_2 = 0.5887$, $\beta_3 = 0.1409$. The $m(\lambda)$ parameter values are $\alpha_0 = 1.2405 \times 10^{-2}$, $\alpha_1 = 3.8474 \times 10^{-5}$. The $k(L^{1/2})$ parameter values are $a = 1.0025$, $w = 20$, and $L_0^{1/2} = 1$. Noise parameters are $\gamma = 10$, $\sigma^2/2\gamma = 35$ and $\sigma_i^2 = 100$.

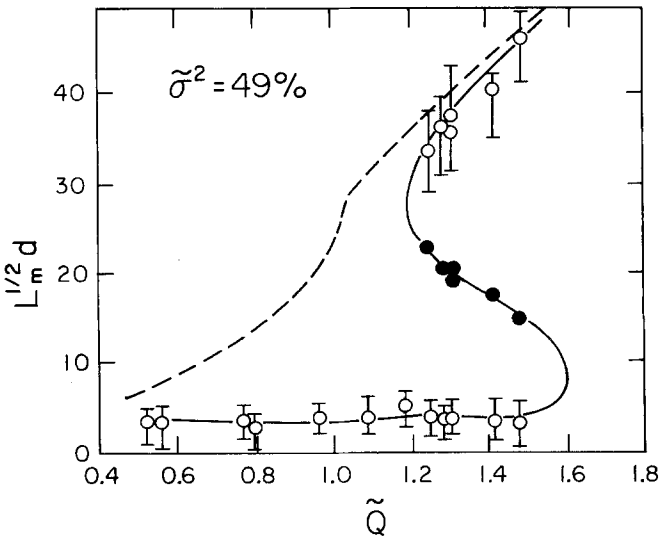

Fig. 4. Bifurcation diagram constructed from extrema of experimental probability densities for $\tilde{\sigma}^2 = 49\%$. Reproduced from Ref. 2.

with Fig. 4 were constructed as a function of L; extrema were found from these and plotted as a function of $L^{1/2}$. These differences taken into account, we note that the locus of extrema in the model has the same hysteresis-curve character as seen in the experimental results of Fig. 4. This is not obtained in the absence of the factor $m(\lambda)$. We find especially suggestive the fact that the model reproduces the curve of maxima in the vortex line density which runs nearly parallel to the $\tilde{Q}$ axis for values of $\tilde{Q}$ under 1.6 in Fig. 4. We offer an explanation for this feature of the experimental data in the next section.

6. PROBABILITY DENSITY NEAR UNSTABLE STEADY STATE

The lower branch of the hysteresis curve in Fig. 4 runs nearly parallel to the $\dot{Q}$ axis. It corresponds to a curve of sharp peaks in the probability distribution at low vortex line density. This result may seem at first thought counterintuitive. One might think that "noise" makes things more random and thus, perhaps, more turbulent. Then we might expect enhanced probability at high vortex line density. However, the explanation for the peak in probability at low vortex line density is quite simple if we think in terms of diffusion processes.

Let us gain a deeper picture of what oblique noise does. Remember that we assumed that the correlation time of the oblique noise was short compared with the typical time scale on which the vortex line density $L^{1/2}$ evolves. Looking back at Fig. 1, we imagine that the system has some particular value of $L^{1/2}$ but that the heat current $\dot{Q}$ is changing rapidly and randomly. The noise is then averaging the vector field of the deterministic system along some horizontal interval in the figure, at a particular value of the ordinate.

When $L^{1/2}$ is small the vector fields in this interval are all fairly similar. The systems which are averaged together remain close to the laminar or unstable steady states, and their drifts (that is, their vector fields, which may point toward increasing of decreasing $L^{1/2}$) are weak. The drift averaged over the horizontal interval then will also be weak, and the diffusion of the noisy system, which depends essentially on the *variance* of the drifts of the averaged systems, will likewise be weak. At the laminar and unstable steady states themselves the oblique noise actually takes us back and forth along the line of steady states. Here all the systems being averaged together have zero drift, and therefore the drift and diffusion contributed by oblique noise is zero. Only the independent noise, which we imagine is relatively weak, keeps these deterministic steady states from also being steady states of the reduced Fokker–Planck equation.

On the other hand, at larger values of $L^{1/2}$ the vector fields are much

stronger. At a particular value of $L^{1/2}$, oblique noise may take us from a point on Fig. 1 close to a turbulent steady state to a point far from one. The drift at the first point would then be weak, and the drift at the second point strong. So the variance of the drifts is also great. Therefore at large $L^{1/2}$ the drift and diffusion terms in the reduced Fokker–Planck equation are large.

For diffusion processes in general, probability tends to concentrate near regions of low diffusion and flow away from regions of high diffusion, unless there is a strong drift which repels realizations from the region of low diffusion. In physical terms we may imagine that oblique noise mixes together states where the vortex line density is increasing and states where it is decreasing. However, if the system happens to visit a state where the total vortex line density is small, it lingers. In such a state the effect of the oblique noise is just to mix it with other states of low vortex line density. On the average, then, as we increase the strength of oblique noise, we visit states of low vortex line density more often and the time spent lingering there increases. The probability density profiles show an enhancement at low values of vortex lines density.

7. EXPERIMENTAL MEASUREMENT OF DRIFT AND DIFFUSION

We shall now describe how to compute finite-difference approximations to the drift $f(L^{1/2})$ and the diffusion $g^2(L^{1/2})$. These two functions are central to the analysis of a diffusion process and make direct contact with the analysis presented in this paper. Suppose that every time a sample path reaches a certain interval of vortex line density $L^{1/2}(t_0) \in (L_0^{1/2} - \Delta, L_0^{1/2} + \Delta)$ with Δ small, the density that occurs an interval of time τ later is recorded. If this is done for a long time series, so that we have many samples that start in the interval of interest, then we could estimate the quantities

$$f_\tau(L^{1/2}) = \tau^{-1} \langle L^{1/2}(t_0 + \tau) - L^{1/2}(t_0) \rangle \tag{7.1}$$

$$g_\tau^2(L^{1/2}) = \tau^{-1} \langle [L^{1/2}(t_0 + \tau) - L^{1/2}(t_0)]^2 \rangle \tag{7.2}$$

where the average $\langle \cdots \rangle$ is taken over realizations for which $L^{1/2}(t_0) \in (L_0^{1/2} - \Delta, L_0^{1/2} + \Delta)$. For a fixed time τ, short compared to the time scales in the interior of the diffusion process, the functions f_τ and g_τ^2 could be plotted as a function of $L_0^{1/2}$.

The drift and diffusion not only characterize the random process in the interior of the state space, but will also give some information on the nature of the boundary conditions. Thus, for the case of natural boun-

daries, where realizations do not actually reach the boundaries,[6,8] both the drift and diffusion will tend to zero as the boundary is approached. For the present case of a reinjection boundary we would first expect f_τ and g_τ^2 to decrease as the laminar boundary is approached, because the laminar state is a steady state. However, sufficiently close to the boundary, the finite size of τ in the finite-difference approximation will begin to become important. Then f_τ and g_τ^2 will begin to increase as the rapid jump away from the boundary begins to influence the average. Finally, very close to the boundary, the contribution from reinjection will dominate the averages, and f_τ and g_τ^2 are expected to approach finite limits whose ratio should characterize the distribution according to which realizations are reinjected into the state space.

The finite-difference approximations to the drift and diffusion could also be used to find the location of the unstable steady state. Here we expect f_τ to decrease to zero while g_τ^2 approaches a finite constant characteristic of the independent noise. These finite-difference approximations can also serve as a check on the fundamental assumption that a diffusion process describes the evolution of the dynamics in the interior of the state space. The estimates of f_τ and g_τ^2 should be independent of τ, for τ sufficiently small, everywhere in the interior of the state space.

8. CONCLUSION

We have introduced a model for superfluid turbulence in the liquid helium counterflow system and in the presence of external noise. The model is based on that previously introduced to describe intrinsic fluctuations in the counterflow system, but has been modified in order to describe the effects of the external noise. These modifications take into account the fact the strong external noise brings global features of the state and parameter spaces into play. The analysis of this model involves a short-correlation-time limit of a nonlinear function of the Ornstein–Uhlenbeck process. We use the generalized white noise limit of Blankenship and Papanicolaou,[5] implemented by means of the wideband perturbation expansion.[6] We also have developed a formula for the probability density corresponding to "reinjection" boundary conditions.

Our model offers a simple explanation for the experimental observation of a sharp peak in the probability distribution corresponding to low vortex line density. We suggest that this peak is associated with the unstable steady state which must lie between the stable laminar and turbulent steady states. Probability concentrates near this unstable state because there the effective diffusion coefficient due to the external noise is very small.

ACKNOWLEDGMENT

M. S. is grateful for the support of the Welch Foundation while a graduate student at the University of Texas at Austin.

REFERENCES

1. W. Horsthemke and M. F. Schumaker, *J. Stat. Phys.*, this issue.
2. D. Griswold and J. T. Tough, *Phys. Rev. A* **36**:1360 (1987).
3. D. Griswold, C. P. Lorenson, and J. T. Tough, *Phys. Rev. B* **35**:3149 (1987).
4. M. F. Schumaker and W. Horsthemke, *Phys. Rev. A* **36**:354 (1987).
5. G. Blankenship and G. C. Papanicolaou, *SIAM J. Appl. Math.* **34**:437 (1978).
6. W. Horsthemke and R. Lefever, *Noise Induced Transitions* (Springer-Verlag, Berlin, 1984).
7. D. Griswold, Ph.D. Thesis, Ohio State University (1986).
8. S. Karlin and H. M. Taylor, *A Second Course in Stochastic Processes* (Academic Press, New York, 1981).